Publication Year	2016
Acceptance in OA@INAF	2020-07-16T10:00:10Z
Title	A first assessment of the strength of cometary particles collected in-situ by the COSIMA instrument onboard ROSETTA
Authors	Hornung, Klaus; Merouane, Sihane; Hilchenbach, Martin; Langevin, Yves; Mellado, Eva Maria; et al.
DOI	10.1016/j.pss.2016.07.003
Handle	http://hdl.handle.net/20.500.12386/26465
Journal	PLANETARY AND SPACE SCIENCE
Number	133

Submitted: Nov 09_2015

A first assessment of the strength of cometary particles collected in-situ by the COSIMA instrument onboard ROSETTA

Klaus Hornung[1], Sihane Merouane[2], Martin Hilchenbach[2], Yves Langevin[3], Eva Maria Mellado[1], Vincenzo Della Corte[4], Jochen Kissel[2], Cecile Engrand[5], Rita Schulz[6], Jouni Ryno[7] Johan Silen[7] and the COSIMA team

(1) Universität der Bundeswehr München, LRT-7, 85577 Neubiberg, Germany, klaus.hornung@unibw.de

(2) Max-Planck-Institut für Sonnensystemforschung, Justus-von-Liebig-Weg 3, 37077 Göttingen, Germany.

(3) Institut d'Astrophysique Spatiale, CNRS / Université Paris Sud, Bâtiment 121, 91405 Orsay, France.

(4) INAF – Instituto di Astrofisica e Planetologia Spaziali, Via Fosso del Cavaliere, 100, 0133, Rome, Italy.

(5) Centre de Sciences Nucléaires et de Sciences de la Matière, Bat.104, 91405 Orsay-Campus,France.

(6) European Space Agency, Scientific Support Office, Keplerlaan 1, Postbus 299, 2200 AG Noordwijk, The Netherlands.

(7) Finnish Meteorological Institute, Climate Research, Erik Palmenin aukio 1, P.O.Box 503, FI-00101 Helsinki, Finland.

Abstract:

Soon after the arrival of the ROSETTA spacecraft at Comet 67/P Churyumov-Gerasimenko the onboard instrument COSIMA began to collect a large number of cometary dust particles on targets of 10 to 30 μm thick gold black. Optical inspection by the COSISCOPE camera subsystem revealed that many of them have an agglomerate structure, consisting of smaller units of typically some tens of micrometers in size. The collection process left the smaller dust particles in an essentially unaltered state whereas particles larger than about 100 μm mostly fragmented upon impact into smaller pieces. Using the observed fragment size distributions, the present paper includes a first assessment of strength for dust particles that undergo disruption upon impact. Most large collected particles have fragmented upon collection at velocities of 2 to 10 m/s. The corresponding weak particle strength (~ 1000 Pa) supports the view that cometary material has undergone very little processing since accretion.

Keywords: Cometary dust, Mechanical strength, Impact fragmentation, Rosetta mission.

1. Introduction:

Interplanetary and cometary dust particles have been collected in the past in various ways where the corresponding decelerations span a vast range of about 12 orders of magnitude. The softest method is by deceleration in the Earth's atmosphere (from some 10 km/s within some 10 km) resulting in some 10^3 m/s^2 and some of these particles get to Earth's surface being essentially unaltered (Duprat et al., 2007, Engrand et al., 2015). Within the STARDUST aerogel collection, deceleration was from 6.1 km/s within some cm target thickness, leading to an order of 10^9 m/s^2, enough to substantially change their shape, but still retaining some of them in solid state (Brownlee 2014). Hypervelocity impact onto a compact silver target within the STARDUST/CIDA instrument produced some 10^{13} m/s^2 enough to vaporize and partially ionize the dust (Kissel et al., 2003). Finally the most extreme setting of hypervelocity impact within the PUMA and PIA instruments onboard the Halley missions (from 80 km/s within the dust's size of μm or even less) resulted in values of up to some 10^{15} m/s^2 leading to complete vaporization of the collected dust as well to substantial single ionization.

The orbital phase of ROSETTA around the nucleus of comet 67P/Churyumov-Gerasimenko made it possible for the first time to collect cometary dust at very low velocities (< 10 m/s in the first months after the rendez-vous, Rotundi et al., 2015). The decelerations of particles on the COSIMA targets are therefore in the range of at most 10^6 m/s^2, just enough to cause mechanical damage upon impact. The present contribution makes an attempt to derive information on the mechanical properties such as strength of the incoming dust from an analysis of the observed damages.

2. Observational data

Since August 2014 the COSIMA instrument continuously exposed its targets to collect cometary dust particles in the coma of Comet 67P/Churyumov-Gerasimenko. The targets consist of metal plates of 1x1 cm^2 from gold, covered by a layer (10 to 30 μm) of gold black, which is a highly porous aggregate (mean density about 2 g/cm^3) consisting of nanometer sized building blocks sticking together by adhesive forces. The metal black layer has been chosen to decelerate and grep the incoming dust for later chemical analysis by secondary ion mass spectrometry (Kissel et al., 2009). The COSISCOPE camera, a subsystem of COSIMA has been designed to locate captured dust particles for the correct positioning of the analyzing ion beam. However, already after a few weeks of COSIMA operation, the images showed such a large number of collected dust particles with such a wealth of morphological details that their independent scientific value became obvious. Those morphological properties are presented in a parallel paper (Langevin et al., 2015).

We report on data obtained during the first half year of data acquisition, from Aug. 2014 to Feb. 2015. In this period ROSETTA was very close to the comet (down to 10 km) and COSIMA collected and identified a total of about 7500 dust particles on two of its target assemblies, D0 and CF, each equipped with 3 gold black targets (named 1D0,2D0,3D0 and 1CF,2CF,3CF). The particles were given individual names as well as a last name (from names of finnish lakes) according to the time period of collection. Their sizes (equivalent diameters) have been found to range between 15 and 400 μm (note the optical resolution of the instrument is 7 ... 14 μm). To provide a first impression Fig. 1a shows a part of target 2CF. One recognizes the general trend that large particles fragment more than small ones. The image also shows that the overwhelming number is in the small size range. Fig. 1b illustrates their size distribution, where the size binning is in steps of 10 μm .

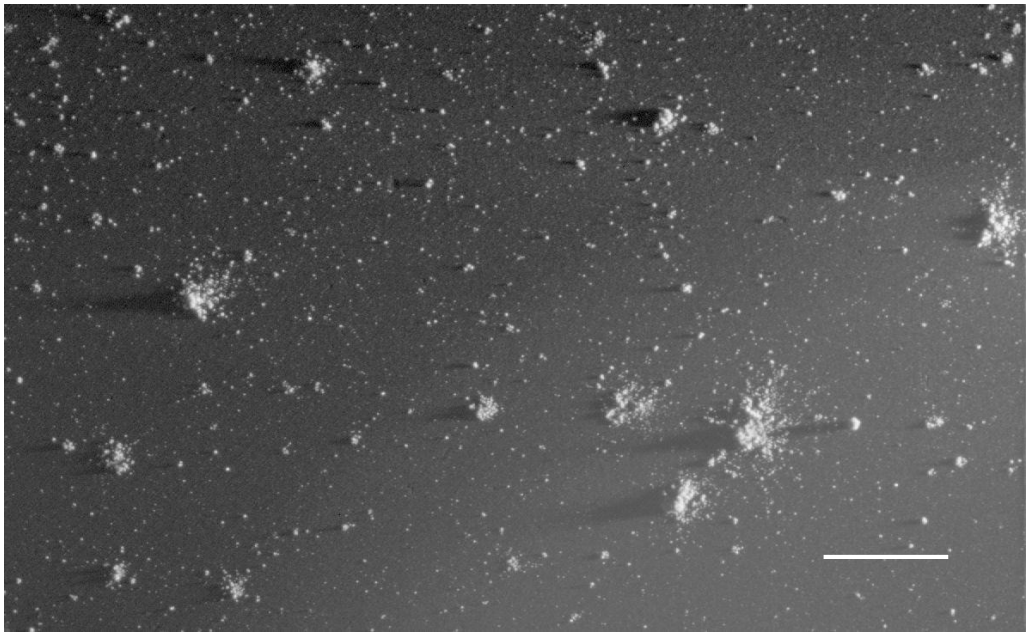

Fig. 1a: A part of target 2CF, status Feb 10, 2015, (scale bar: 1 mm).

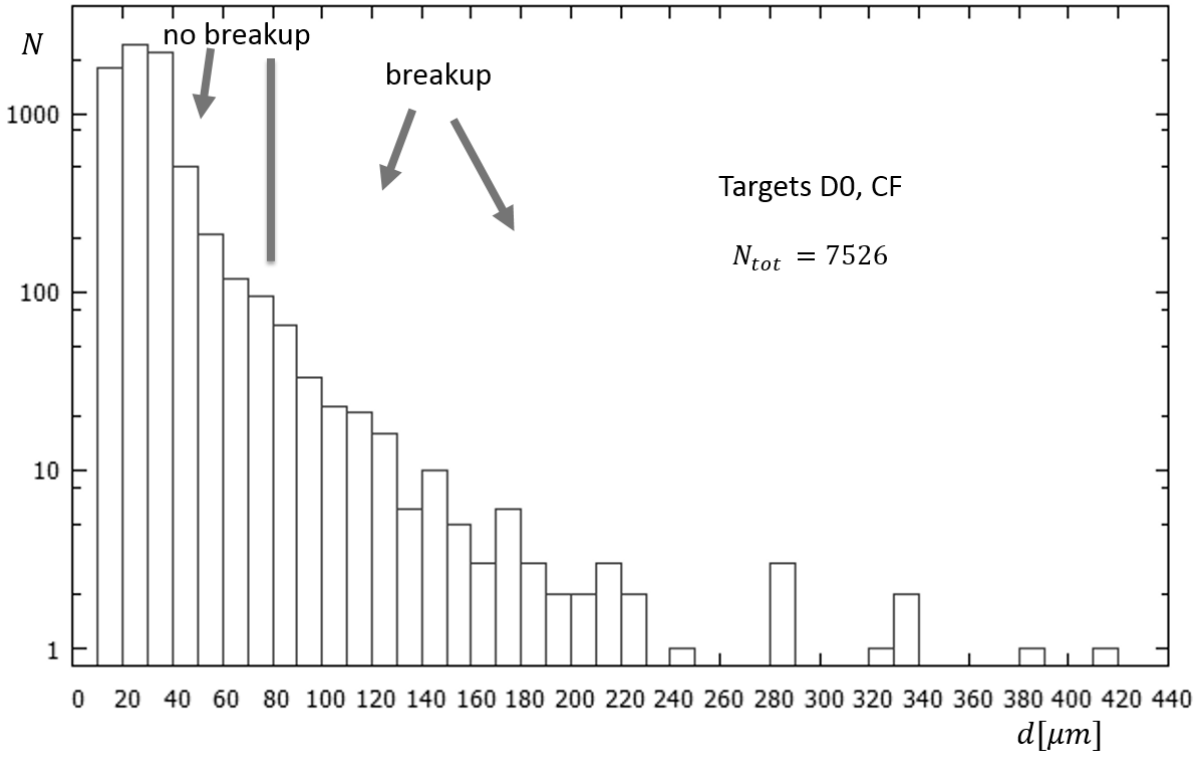

Fig. 1b: Size distribution of dust particles for the collection period from Aug. 2014 to Feb. 2015 with an indication of approximate location of the breakup boundary (N = number per $10\ \mu m$ interval; $d = \sqrt{\frac{4}{\pi} \cdot a}$, a= area in image plane).

Enlarged images of selected areas on the targets have been used for analysis. The images shown in section 2.2 have been produced with a spatial resolution of slightly less than 10 μm, which has been achieved by combining 4 individual 14 µm pixel-size images shifted by half a pixel in the X or Y direction. Illumination is under grazing incidence. In the images below the illumination is from the right side and they are displayed in log-scale. For details of the imaging, see Langevin et al. (2015).

Already a quick look at the enlarged images (Figures 2 below) shows that most of the collected dust particles present themselves as cluster-like aggregate structures consisting of individual sub-units in the order of some tens of μm in size, reminiscent of a "bunch of grapes" (see Figures 2a, 2b below). For clarity we will denote these sub-units by "cluster elements" or simply "elements" in the remainder of the paper. Those elements may consist themselves of smaller units down to sizes of some 100 nm (a size range which is accessible to the MIDAS instrument onboard ROSETTA, Riedler et al., 2007, Bentley et al., 2014). Interplanetary dust particles (IDP's) collected in the upper atmosphere show such an extension of sub-structure down to sub-µm scales (Brownlee, 1985). The second finding from optical inspection is that the collected dust did not seem to penetrate much into the black layer but often stays at its surface as can be seen from the long shadows indicating a height which is in some cases even comparable to its lateral dimension. Some particles stick out of the targets, the contact area with the black substrate being small in relationship to their size, as shown in Langevin et al. (2015). This led to the assumption that the impact velocities might be very low. A quantitative confirmation came from the GIADA instrument onboard ROSETTA which directly measured velocities with high precision to be less than about 10 m/s (Rotundi et al., 2015, Della Corte, 2015).

2.1. Fragmentation categories

According to the degree of damage upon impact we categorize the breakup events into 3 groups: a) "no breakup", i.e. no damage visible. b) "simple breakup", i.e. breakup into few smaller fragments, which stay close together, c) "catastrophic breakup" into many fragments much smaller than the parent dust connected with an ejection of fragments into the neighbourhood, leaving finally a "rubble pile" as remnant at the center. For most cases the largest particles are of type c). An example is Nilda, Fig. 2a-5. Intermediate sized ones are mostly of type b). Examples are Stefanie and Pertti (Fig. 2a-3, 2a-4). Pertti does show some fragments in the neighbourhood, which puts it closer to the catastrophic case. No breakup, type a), mainly occurs for small particles. Example is Pecine (Fig. 2a-2). However, there are also cases where large dust particles do not fragment, like Lambert (Fig. 2a-1). These might be the candidates for large compact dust, i.e. they would probably be less porous than most of the larger dust particles and possessing a higher strength (Rotundi et al., 2015, Langevin et al. 2015).

2.2 Special phenomenon: shedding of fragments from a stronger core

A phenomenon, shedding (Clark et al., 2004) has been detected in some cases. An example is Jean-Baptiste, Fig. 2b-10. The image shows a compact looking central part, surrounded by small fragments. The phenomenon may be explained by a stronger core which has some loose elements sitting at its surface which are detached by the impact, but the central part is non-fragmenting. This then might be an indication that a compact core is present with higher strength than the fragmenting dust.

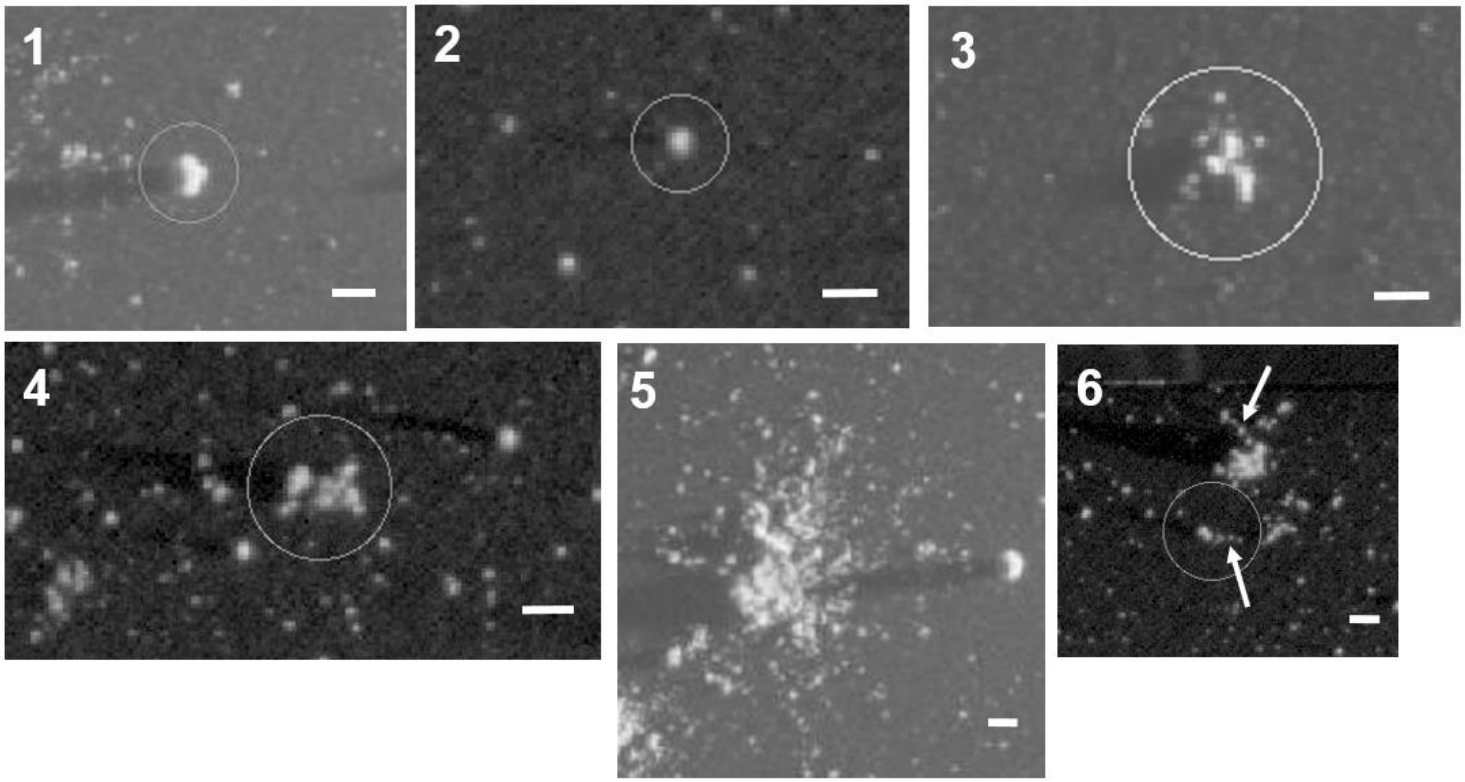

Fig. 2a : 1: no breakup: 2CF Lambert Kolima.3, d ≈ 110 μm, h≈ 116 μm.
2: no breakup: 1CF Pecine Ala Kitka, d ≈ 45 μm, h≈ 50 μm.
3: simple breakup: 3D0 Stefanie Saimaa, d ≈ 100 μm, h≈ 40 μm, fragment sizes 15-35 μm (diameter).
4: simple breakup: 2CF Pertti Kolima.3, d ≈ 130 μm, h≈ 50 μm, fragment sizes 20-35 μm.
5: catastrophic breakup: 2CF Nilda Kolima.3, d ≈ 410 μm, h≈ 120 μm, fragment sizes 10-30 μm.
6: shedding by rolling: 2CF Clarence Kolima.3, d ≈ 70 μm, h≈ 25 μm, fragment sizes 10-20 μm.

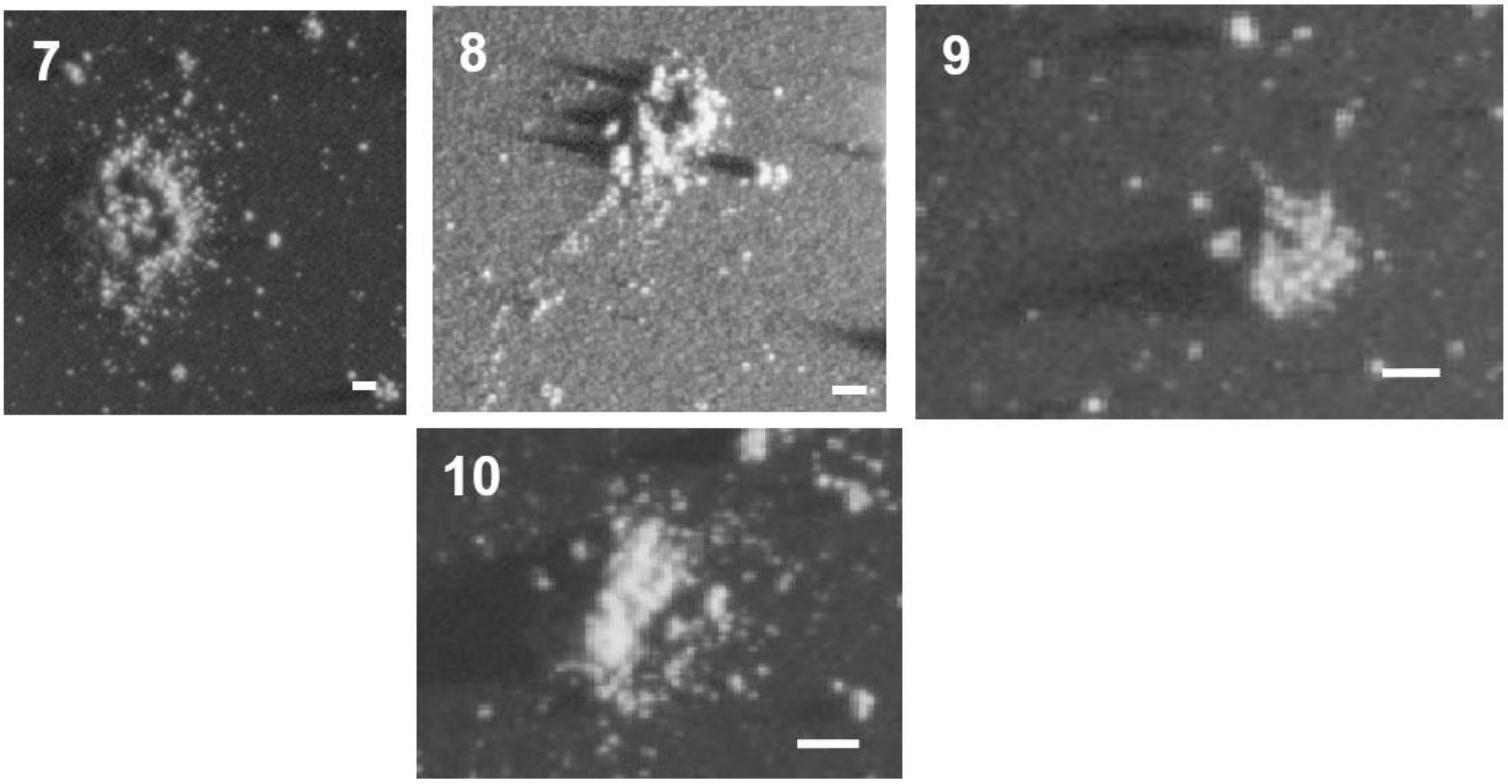

Fig. 2b: 7: depression at center: 2CF Jessica Lummene.2, d ≈ 380 μm, h≈ 50 μm.
8: depression at center: 3D0 Kamil Ukonvesi, d ≈ 225 μm, h≈ 60 μm.
9: linear chains of elements: 2CF Adeline Kolima.3, d ≈ 190 μm, h≈ 50 μm, element sizes ≈ 20 μm.
10: shedding from a stronger core: 2CF Jean-Baptiste Kolima.3, d ≈ 340 μm, h≈ 127 μm, element sizes ≈ 20-30 μm.

$d = \sqrt{\frac{4}{\pi} \cdot a}$, a= area in image plane, h= height as derived from shadow. All scale bars = 100 μm.
Collection periods of examples shown: (date of begin+days of exposure):
Kolima.3 (01/24/2015+1.0); Ala Kitka (12/16/2014+3.7); Saimaa (10/29/2014+4.7);
Lummene.2 (01/26/2015+1.0); Ukonvesi (11/10/2014+4.0).

2.3 Special phenomenon: shedding of fragments by rolling

Some fragments seem to roll along the target surface for a certain distance as can be seen from Fig. 2a-6. The rotational movement probably has two sources: 1.The incoming dust is touching the inclined walls of the collecting funnel placed in front of the target assembly where translational energy is transferred to rotational energy by friction. 2. In large impacts, which lead to a central “rubble pile” (Nilda, Fig. 2a-5) outer parts of the pile may roll “downhill” in the inertial field of deceleration which acts in the same way as a gravitational field (which is, of course, missing in our case). Again friction converts translation into rotation. During subsequent rolling along the target surface a large fragment may lose smaller parts on its way until it comes to rest. There are some examples for this phenomenon in the images. Large impact sites are surrounded by radial traces of small fragments forming a neat straight chain of small fragments away from the impact site (e.g. Nilda, Fig. 2a-5). Again the sizes of these fragments are “standard”, i.e. in the order of some tens of μm. At the end of this chain there is often a larger “residual” particle (see Fig. 2a-6).

2.4 Special phenomenon: central depressions

Normally large impacts end up with a central pile and fragments around. However, there are few examples where it is the other way round: in the center there is a hole, or more precisely a shallow depression (examples Jessica Fig. 2b-7 and Kamil Fig. 2b-8). An incoming dust aggregate, consisting of a compact central core, covered with standard fluffy material might produce such a pattern. Upon impact the outer parts of the compact core are shed off producing a ring pattern of fragments, while the central particle may rebound off the target. Larger pieces of ices wrapped in a layer of minerals, which is removed by the impact and subsequent sublimation might also be an explanation (mineral covered ices instead of the present model of ice covered minerals, e.g. Greenberg and Hage, 1990). If this would be the case, it would have consequences for our understanding of the way ices and dust co-exist inside the comet.

2.5 Chain structures

Linear chains of cluster elements sometimes become apparent. An example is Adeline, see Fig. 2b-9. It is an indication of high porosity, since the formation of a cluster where each element touches at least two others needs low dimensionality in the inner architecture of the ensemble. The discovery of such structures in the data is significant, since it gives an argument for an approximate model description, which is performed in Sec. 3.3.

2.6 Size distribution of cluster elements

Fig. 3 shows the size distribution of fragments for a larger number of fragmenting dust particles in order to improve statistics. The identification of small dust as fragments belonging to a certain parent dust particle is done in an empirical way by optical inspection. Mostly they are found within a few radii from the central cluster. Furthermore, by analyzing fragments as well as inspecting the “elements” of not-fragmented parts, almost identical sizes are found (about 15 – 40 μm in diameter). This is an important finding which suggests that the fragments are not formed during the impact process, but pre-existing in the composite particle. The impact is simply tearing them off the parent dust particle. For the modeling in Sec. 3.3 we will need only the slope of the distribution of Fig. 3.

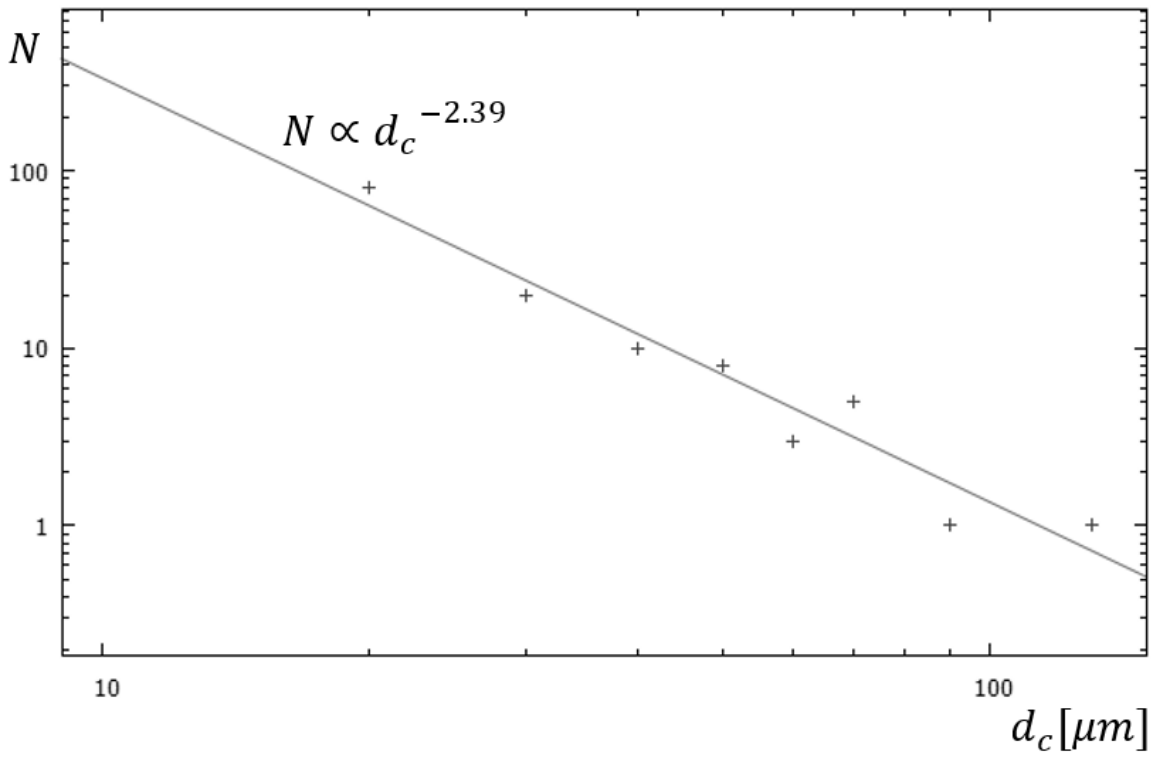

Fig. 3: Fragment size distribution from various impacts with breakup:

1CF Valerie Enonvesi, 1CF Tolja Enonvesi, 2CF Landry Ala-Kitka, 2CF Herve Inari, 1D0 Sigrid Vesijako, 1D0 Hanna Hankavesi, 2D0 Nyle Nilakka, 2D0 Alizee Nilakka, 3D0 Kamil Ukonvesi, 3D0 Arvid Saimaa, 3D0 Eloi Saimaa.

$d_c = \sqrt{\frac{4}{\pi} \cdot a}$, a= area in image plane). $N =$ number of particles per $10\ \mu m$ size bin.

Collection periods (date of begin+days of exposure): Enonvesi (12/20/2014+6.6); Ala-Kitka (12/16/2014+3.7); Inari (01/02/2015+6.7); Vesijako (11/17/2014+4.0); Hankavesi (08/25/2014+6.4); Nilakka (09/29/2014+7.0); Ukonvesi (11/10/2014+4.0); Saimaa (10/29/2014+4.7).

2.7 Summary of observations

a) Breakup depends on size: small particles below about 80 μm do not fragment, whereas those above 100 μm in most cases are fragmenting (except a few, like Lambert, Fig. 2a-1) and in the zone between both behaviors can be observed. b) The spectrum of fragment sizes is rather narrow: most of the fragments are between 15 and 40 μm. c) In many cases of large particle impacts there is a central pile of material but with a clear agglomerate structure whose elements have sizes comparable with those of the isolated fragments which have been detached from the parent dust. This led us to the tentative conclusion that the breakup tears apart pre-existing elements. d) Fragments are distributed up to several 100 μm away from the impact site which may be explained by a kind of movement during which the contact with the surface is maintained, since there is no gravity which hold them attached to the surface and one possible interpretation may be rolling.

3. An estimate of mechanical strength from breakup observation

Strength of cometary matter has been investigated with the focus on comet formation (Blum et al., 2008, Güttler et al. 2009, Blum et al., 2014). In our case the focus is on the state of the material, which has been processed during passage close to the sun and also after liftoff from the cometary surface when the volatiles successively sublimate (Clark et al., 2004) to become the very light material we see in our collections (Schulz et al 2015).

To derive strength from the observed breakup behavior, we cannot make use of the classical theories (Thomson 1973) since no data are available for material properties like Young modulus, surface tension etc. Methods more tuned to low density accreted materials start from very small building blocks of sub micrometer scales (Blum et al. 2014). Breakup is then simulated numerically by detailed modeling of grain interactions. The results agree well with laboratory experiments of fine dust of known material properties (e.g. SiO_2). Application to "real" cometary dust depends on information on the physical nature of the smallest sub micrometer building blocks. Probably they consist of a mixture of minerals, embedded in non-volatile organic material or glasses (Matrajt 2012,Bradley 2012, Engrand 2015) forming a relatively strong grain, but little is known about their mechanical properties. In view of this situation we use in our data interpretation simplified modeling concepts with the aim to derive limits for strength. Due to the simplicity of these concepts we will not distinguish between compressive, tensile and shear strength. Also, when discussing strength one has to keep in mind that it depends on the process the material undergoes (Housen and Holsapple 1990). Suppose we put our dust into a ball mill where high strain rates are produced, then the relevant strength would be much higher than within the present impacts and much smaller substructures would be involved.

3.1 Constraints for strength from energy density

We use a simplified criterion by assuming that breakup happens if the impact induced energy density (mechanical energy per unit volume) exceeds the internal strength. Similar simplified ways of reasoning have been applied for instance to treat hypervelocity impact of a projectile into a larger target body (Housen and Holsapple, 1990), or the aerodynamic deceleration during atmospheric entry of meteors (Ceplecha and McCrosky 1976) or the action of differential gravitational forces as in the case of Shoemaker-Levy 9 breakup during the 1992 Jupiter passage (Scotti and Melosh 1993). In our case the incoming dust particle is assumed to dissipate its whole kinetic energy during the impact and therefore the mechanical energy density is proportional to the dust particle's mass density ρ and the square of the velocity v :

$$\sigma_{ed} = \frac{\rho}{2} \cdot v^2 \qquad (1)$$

In terms of continuum mechanics this would correspond to the pressure increase at the stagnation point. In atmospheric entry the expression is almost the same (apart from a factor of two), ρ being the air density at high altitudes and velocities of several km/s are required for meteoritic breakup. In our case ρ is the orders of magnitude higher solid state density of the dust particle and this is the physical cause why velocities of some m/s are sufficient for breakup. Eq.(1) suggests that a size dependent density is required to explain the fact that large dust particles break up more easily than small ones. Explaining the effect with different velocities would require assuming that large dust particles are faster than small ones which is difficult to imagine.

Dust particle velocities for the time of observation (Aug. 2014 to Feb. 2015) have been measured by the GIADA instrument onboard ROSETTA and we take the values reported by Rotundi et al., 2015, Della Corte et al., 2015 by assuming that the dust particles we observe have similar velocities. This provides an evaluation of the velocity distribution with a mean value of 3.5 m/s and a width of +- 1.5 m/s. An estimate of the porous density requires care and an awareness of a possible large error. We tentatively assume an approximate power law:

$$\rho = \rho_0 \cdot (r/r_0)^{-b} \qquad (2)$$

To define the constants we start from the smallest units of an order of 0.1 μm in radius size assuming them to be compact. We further assume that the volatiles have sublimated (with possible exceptions as discussed in Sec. 2.4), i.e. minerals and refractory carbon-rich organics are left whose mean density we estimate to about 2.5 g/cm^3 based on the composition estimates of Greenberg and Li (1999). It is interesting to note that this value is in good agreement with the evaluation by Rotundi et al. (2015) of the density of compact dust measured around the nucleus of Churymov-Gerasimenko (1.9 +- 1.1 g/cm^3). Further information can be drawn directly from our images of not-fragmented dust agglomerates, see e.g. the particles of Fig.2b) 7,8 and 9. They look far from being as porous (0.15 fill factor) as postulated by Blum and Schräpler (2004) but also far from close packed (fill factor 0.74). Assuming an intermediate value of the fill factor (~ 0.4) would lead to a density decrease by a factor of 1/0.4 = 2.5 per decade of size since the individual elements in the images have a size of roughly 1/10 of the parent dust particle. Applying this also to the sub-micron grains would result in $\rho = \rho_0 \approx 1$ g/cm^3 at $r = r_0 \approx 1$ μm which is consistent with densities determined in the coma of Halley (Maas et al., 1990, Hornung and Kissel 1994). For dust in the order of 100 μm in radius a density of 0.16 g/cm^3 would then be reached. This is already less than the comet's mean density (about 0.4 g/cm^3). This is in line with our supposition that the dust we are seeing most probably has lost its volatiles and has been intensively processed at the surface of the comet before its liftoff (Schulz et al, 2015). We use this law for an extrapolation up to a few 100 μm, but one should not extrapolate further. Fig. 4 shows the resulting energy density σ_{ed} in dependence on velocity for various values of the mass density ρ .

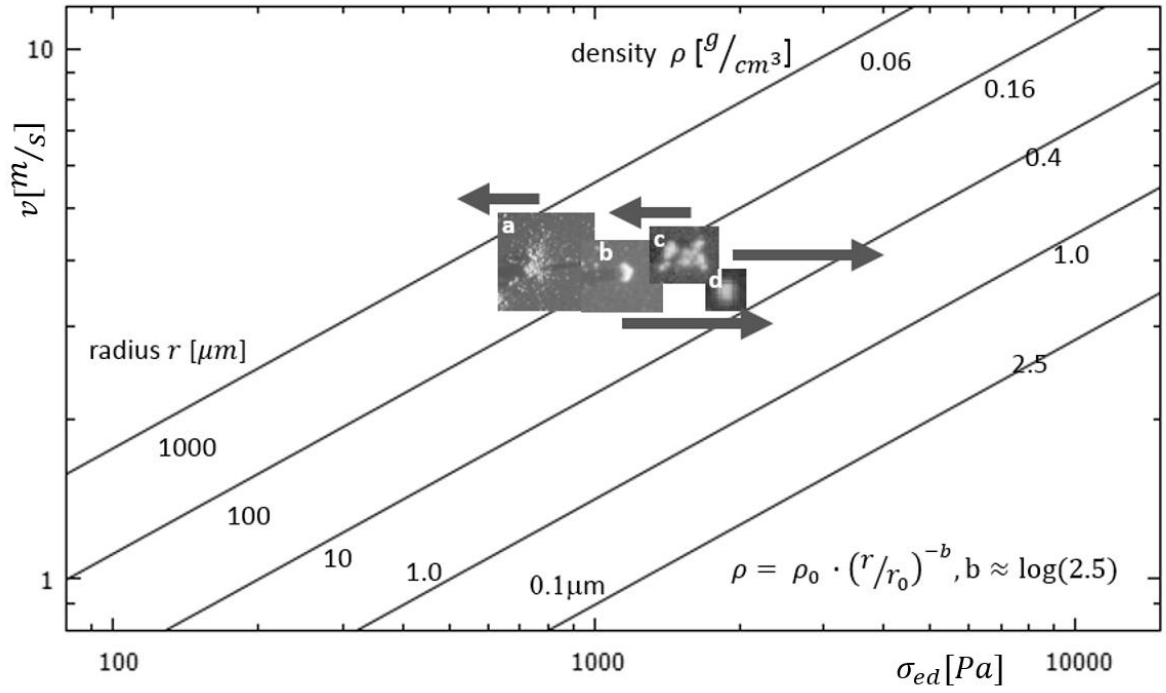

Fig. 4: Energy density σ_{ed} in dependence on collection velocity v for various mass densities ρ of the impacting dust particle together with the possible location of particles of Fig. 2.a: Nilda, b: Lambert, c: Pertti, d: Pecine.

The above energy density argument leads to the following constraints for particle strength:

a) Catastrophic breakup, e.g. Nilda. Its position is indicated for the estimated velocity interval and densities from Eq. (2). For fragmenting particles such as Nilda, the energy density value gives an upper bound for the strength. For Nilda strength values less than ~1000 Pa result.

b) The simple breakup events show similarities with the catastrophic break-up events. The main difference is that the incoming dust has a smaller size (by a factor of 4 for the examples of Fig. 2a) and therefore a higher density (Eq. 2) hence breakup results in only a few fragments. The resulting position for 2CF Pertti as shown in Fig. 4 indicates that the upper limit of its strength should be slightly higher than ~1000 Pa.

c) When there is no breakup, the energy density value provides a lower limit to the strength of the particle. The corresponding position of 1CF Pecine in Fig. 4 shows that its strength should be higher than about 2000 Pa. The size of Pecine (about 40 μm) is already down to the size of typical elements within larger dust particles (and also of their fragments upon impact) such that its non-breakup appears logical. Much higher impact velocities would be needed to further break up these small particles. The same argument holds for larger non-fragmenting dust particles like 2CF Lambert.

Recently the possibility of extremely low densities of about 1 kg/m^3 has been proposed and discussed: For these particle detections, very low velocities, down to 0.1 m/s, were observed by GIADA, but these observed particle velocities could be specific to GIADA (Fulle et al., 2015). The low particle velocities are explained by particle deceleration by electrostatic forces between the charged particles and Rosetta spacecraft surface potentials, which could be different for each instrument. For this reason COSIMA might not collect such slow dust particles on its targets since the targets are located well within the spacecraft behind a 0.15

m long dust collimator with a field-of-view of 15° x 23°. This could result in a selection effect when the Rosetta spacecraft velocity is perpendicular to the dust velocity. Should the velocities of low density, high material strength particles within COSIMA be larger than about 30 m/s they could also reach the target and break up upon impact onto our targets.
The issue, however, needs further clarification. On our images, up to now, we do not see indications for such big changes in morphology that could contain density changes between 2 and 3 orders of magnitude (Langevin et al., 2015). Instead we observe a rather steady transition from compact dust ("breccia") to "clusters" which in some cases look more rigid ("glued clusters") or show beginning signs of breakup ("shattered cluster") or finally the ones which break up catastrophically ("rubble piles").

d) When there is "shedding from a stronger central core" this indicates that the particle might not be homogeneous in strength (e.g. Jean-Baptiste, Fig. 2b-10). From the size of the fragments in the neighborhood one would assume a loose outer part, with a strength being comparable to the case of fragmenting dust and an inner core comparable to the case of compact dust ("glued cluster" Langevin et al. 2015).

e) Shedding by rolling: Also in this case the detached fragments have approximately the same sizes. However, one also observes detachment from small parent particles, e.g. 2CF Clarence Fig. 2a-6 which can be explained by a stronger adhesion force with the target's black than the forces between the dust's elements since the gold black layer has a much smaller fine-structure.

The estimated numbers hold for the assumed velocity interval of a few m/s. The resulting strength bounds change if we assume larger variations in v. For example the fact of non-fragmentation of some large dust particles may be explained by high strength, but also by low impact velocities. And if the velocity would be higher, then the upper bound for the energy density of fragmenting dust simply would shift upward (see the examples in Sec. 3.5).

3.2 Constraints for strength from deceleration forces

Another contribution to the issue of strength can be derived from an estimation of the forces occurring during deceleration. The experimental setting of COSIMA can be regarded as a "controlled impact experiment in space" (Fig. 5).

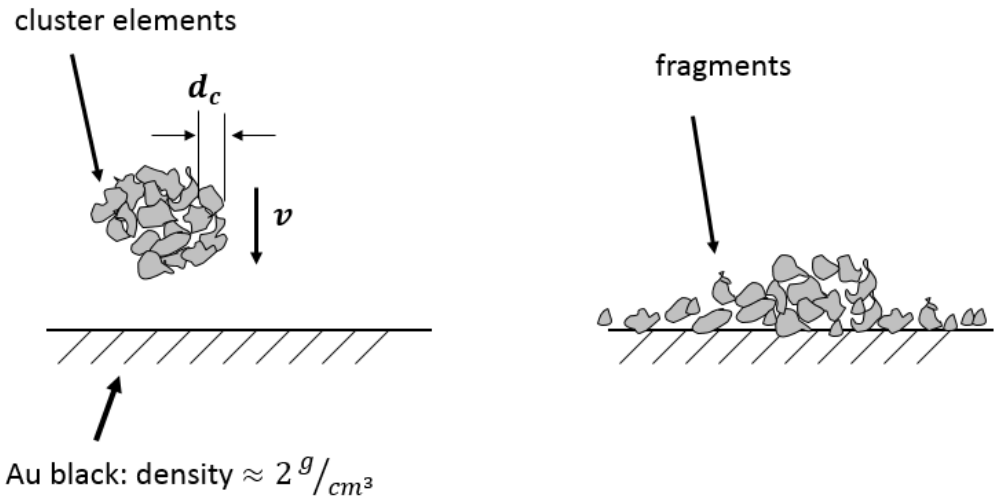

Fig. 5: An impact fragmentation experiment in space.

Consider an individual cluster element "c" . It is attached with a certain binding force to the parent agglomerate and for the moment being let us assume that this force is proportional to the cluster element's size:

$$F_{bind} = C \cdot d_c \qquad (3)$$

To tear the element off the parent agglomerate, the inertial force by deceleration from velocity v to zero velocity within a certain breaking length s has to be larger than the binding force:

$$F_{dec} = m_c \cdot \frac{v^2}{2s} = \frac{\pi {d_c}^3}{6} \cdot \rho_c \cdot \frac{v^2}{2s} \; > \; F_{bind} \qquad (4)$$

For the breaking length s we can take advantage that we know the approximate surface structure of the collection substrate (porous gold, see Hornung et al., 2014) which shows a typical roughness in the order of $10\ \mu m$, see Fig. 6 and we take this value as an estimate for s . We further assume that the size dependence of the density as described by Eq.(2) also holds for the density ρ_c of the individual cluster elements.

For the force constant C in Eq. (2) we take a lower limit, derived from van der Waals interaction: $C = \frac{A}{24 \cdot D^2}$, $D \approx 0.4\,nm$ using the Hamaker constant of dry minerals $A \approx 10^{-19}\,J$ under vacuum conditions, leading to $C = 2.6 \cdot 10^{-2}\,N/m$ (Israelachvili, 2011).

The resulting values for the deceleration and binding forces are shown in Fig. 7 for various impact velocities around the mean value of 3.5 m/s. The crossover between binding and deceleration forces then defines the lower limit of fragment size, which can be detached from a parent bigger dust aggregate (between 10 and 15 μm). From our optical inspection we do have indication that much smaller fragments are absent. However, since 10-15 μm is close to our optical resolution of 10 μm an independent confirmation would be helpful. It comes from our SIMS measurements (Hilchenbach et al., 2015). If smaller dust fragments would be present, then they would contribute significantly to the SIMS signal also in the spaces between the locations where we detect dust fragments, since SIMS is sensitive to surface coverage only. The fact that we see a clear change of the ion signal from “on the dust” to “off dust” down to background values gives further evidence that we do not miss many smaller fragments. From this agreement of calculated and observed minimum fragment sizes we tentatively conclude that the assumption of van der Waals interaction is reasonable and we will use this finding in the next Section.

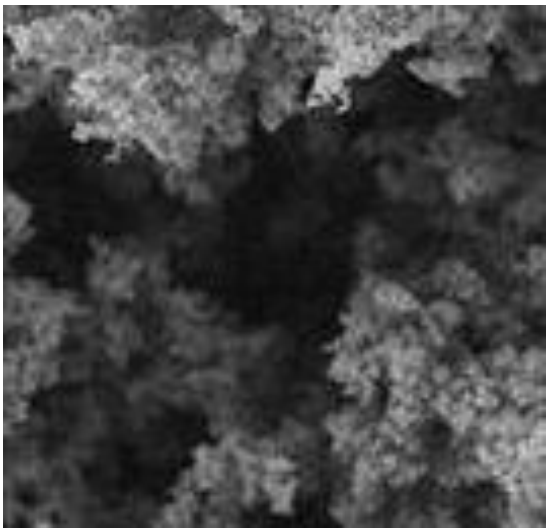

Fig. 6: Surface structure of Au black (SEM image: 8x8 μm^2). The scale of this image is smaller than a single COSISCOPE pixel (14 x 14 μm^2), and Au black appears quite smooth at COSISCOPE image scales.

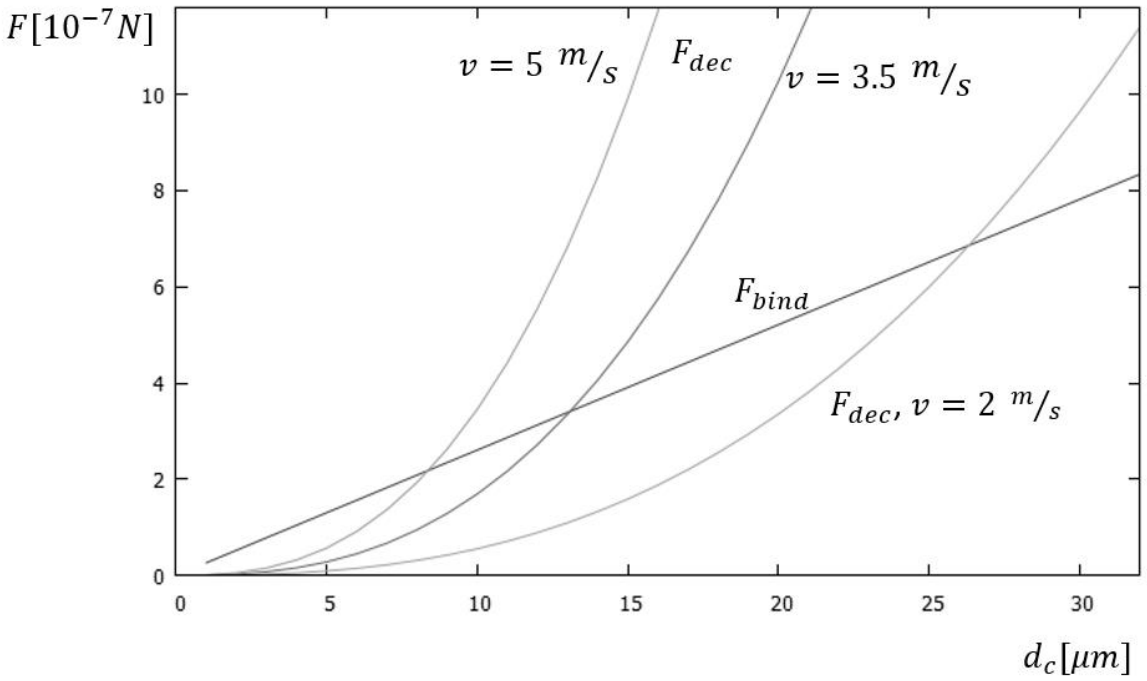

Fig. 7: Size dependence of forces: The crossover point defines the minimum size of elements which can be detached by the impact from the parent dust particle (examples $v \approx 2, 3.5, 5\ m/s$).

An additional application for forces is an estimate for rolling distance of fragments along the target away from the impact site (Sec. 2.3). Since there is no gravity, they can be attached to the gold black surface only by adhesion, which is roughly twice as large as the inter-particle force: $F = 2 \cdot C \cdot d_c$ (Israelachvili, 2011). The rolling resistance generally is less than the normal force by some factor, known as "rolling resistance coefficient" c_{rr} , a quantity which in technical systems lies between 0.01 and 0.1 (Bower, 2010). Assuming that the whole impact energy is transferred into rotation we estimate the rolling distance for a $d_c = 20\ \mu m$ fragment (using density from Eq.(2)) to be: $\Delta x = \frac{\frac{m}{2} \cdot v^2}{F \cdot c_{rr}} \approx\ 100 \ldots 1000\ \mu m$ for $c_{rr} = 0.1 \ldots 0.01$. The observed movements of fragments away from the impact site are in the order of a few 100 μm (see Fig. 2a-6).

In the present discussion of forces there was no distinction whether the tearing force is a normal one or is partly in shear direction, which is reasonable for dust with high porosity. For example Kirchner et al. (2002) measured both tensile and shear forces for low density dry snow at $\rho \approx 0.17$ g/cm^3 and found no difference.

3.3 Estimating strength of the incoming dust from its fragment size distribution

We now undertake an effort to characterize the strength of the incoming dust particle, having a mean density ρ , from its fragments. Assume we split a parent incoming dust particle in two parts along an imaginary dividing surface. Then the strength would be defined as the force necessary to tear them apart divided by the area of the dividing surface:

$$\sigma = F_{bind} \cdot n_c \cdot d_c \ , \ n_c = \frac{\rho}{m_c} \qquad (5)$$

where $n_c \cdot d_c$ is the number of cluster elements per unit area at the dividing surface. The observed chain structures within not-fragmented dust supports such simple ways of reasoning. As a lower bound we assume for F_{bind} van der Waals interaction Eq.(3) and get (now switching to radius for formal reasons):

$$\sigma = \frac{3}{\pi} \cdot C \cdot \frac{\rho}{\rho_c} \cdot \frac{1}{r_c} = \frac{3}{\pi} \cdot C \cdot \emptyset \cdot \frac{1}{r_c} \qquad (6)$$

This equation shows the basic dependence of the strength on various parameters, σ being proportional to the volume filling factor $\emptyset = {}^{\rho}/_{\rho_c}$ and inversely proportional to the size of the cluster elements making up the dust. It is however over simplified since it assumes uniform cluster element sizes. If a pair of two cluster elements has different radius r_c, r_c' then the van der Waals binding force is: $F_{bind} = 2C \cdot ({}^{2r_c r_c'}/_{r_c + r_c'})$ (Israelachvili, 2011). When applying to a spectrum of sizes, $f(r_c)$ one has to sum the contributions of the pairs of elements contained across the imaginary dividing surface:

$$\sigma = \sigma_0 \cdot \frac{\int_{r_{c_1}}^{r_{c_2}} f(r) \cdot r \cdot \left\{ \int_{r_{c_1}}^{r_{c_2}} f(r') \cdot \frac{2rr'}{r+r'} dr' \right\} dr}{\int_{r_{c_1}}^{r_{c_2}} f(r) \cdot \frac{\rho_c(r)}{\rho_0} \cdot r^3 \, dr} \ , \qquad (7)$$

where:

$$\sigma_0 = \frac{3}{\pi} \cdot C \cdot \frac{\rho}{\rho_0} \cdot \frac{1}{r_0} \quad ; \rho_0 = 1000 \frac{kg}{m^3}; \ r_0 = 10^{-6} \, m$$

Integration goes over the measured fragment size range: $r_{c_1} < r_c < r_{c_2}$. $f(r_c)$ is the size distribution:

$$f(r_c) = a \cdot r_c^{-c}, \qquad c \approx 2.39 \ , \qquad (8)$$

where the constant c is taken from the data of Fig. 3. Normalization to one within the observed size range gives: $a = (1-c)/(r_{c_2}^{1-c} - r_{c_1}^{1-c})$, i.e. we assume that within the fragmenting dust particle those parts contribute to the strength which show up in the

fragment spectrum. The size dependence of the cluster element densities ρ_c is taken from Eq.(2).

It might be of interest to check the volume filling factor ∅ for the multi-size case, because there are narrow limits for it (e.g. it cannot exceed 0.74 and hardly go below 0.1). It is given by the ratio between the incoming parent dust mean density ρ and the cluster element density $\overline{\rho_c}$ averaged over the size spectrum:

$$\emptyset = {}^{\rho}/_{\overline{\rho_c}} \quad , \quad \overline{\rho_c} = \frac{\int_{r_{c_1}}^{r_{c_2}} f(r)\cdot\rho_c(r)\cdot r^3 dr}{\int_{r_{c_1}}^{r_{c_2}} f(r)\cdot r^3\, dr} = \left(\frac{4-c}{4-c-b}\right)\cdot\left(\frac{{r_{c_2}}^{4-c-b}-{r_{c_1}}^{4-c-b}}{{r_{c_2}}^{4-c}-{r_{c_1}}^{4-c}}\right) \qquad (9)$$

Eq.(9) describes the packing density of the cluster elements, which themselves are thought to be porous with respect to the smallest sub-micron building blocks of the material.

Resulting numerical values for strength σ and volume filling factor ∅ for a large impacting dust particle (example: radius 100 μm, mean density ρ of 0.16 g/cm^3) are given in Table 1 for various combinations of minimum and maximum fragment sizes r_{c_1}, r_{c_2} and Fig. 8 illustrates the shape of the solution of Eq.(7). The strength values are in the order of 10^3 Pa, which is close to the values which has been measured for dry snow (≈ 770 Pa at a density of $\rho \approx 0.17$ g/cm^3 , see Kirchner 2002) and also close to the values derived from simulations and experiments with sub-micron building blocks (Güttler et al. 2009).

$r_{c_1}[\mu m]$	$r_{c_2}[\mu m]$	$d_{c_1}[\mu m]$	$d_{c_2}[\mu m]$	∅	σ/σ₀	σ [Pa]
5	20	10	40	0.43	0.1952	776
5	10	10	20	0.36	0.2890	1150
1	20	2	40	0.40	0.1410	560
1	10	2	20	0.31	0.2605	1036
1	5	2	10	0.25	0.4429	1762

Table 1: Example values of Eq. (7) for various size bounds as well as resulting strength values for a mean density of 0.16 g/cm**3 corresponding to a r = 100 μm sized parent incoming dust particle (σ_0 = 3973 Pa).

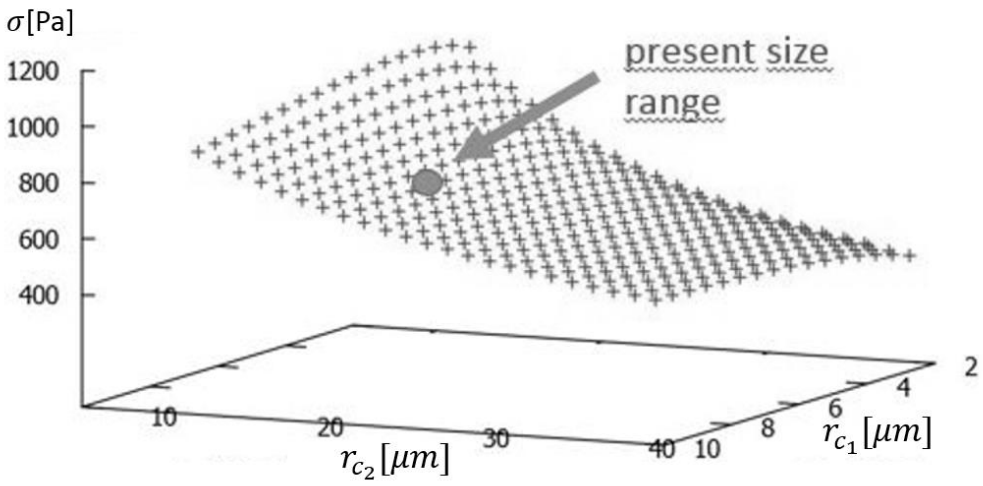

Fig. 8: Mechanical strength [Pa] in dependence on fragment sizes for the example of ρ= 0.16 g/cm^3 σ_0 = 3973 Pa. Every point on the plotted surface corresponds to a window of lower and upper sizes and the window found in the images is marked.

3.4 Sensitivities and errors

It is important to check the sensitivity of the determination of strength on the different input parameters. This is shown in Table 2 for possible deviations from an example reference state. It is interesting to see that the largest fragment r_{c_2} influences strength much more than smallest ones r_{c_1} (see also Fig. 8). This is an important help for the present data reduction, since the COSISCOPE camera's resolution is limited at small sizes to ≈10 μm (see Langevin et al., 2015), which means that if we would miss smaller fragments down to a few μm the resulting strength would not change much. Also the steepness c of the size distribution does not play a major role, which is a justification for choosing the mean value determined from a large number of collected particles (Fig. 3). One of the remaining players in the game is the interaction force constant C .The value chosen is for mineral materials and may be lower by a factor of two for refractory organics (Israelachvili 2011). However our data analysis on forces (Sec. 3.2) suggests values close to the mineral value. The volume filling factor $\emptyset = \rho/\overline{\rho_c}$, Eq.(9) enters through the steepness b of the size dependence of the density (Eq.(2)). There is a linear dependence of strength on the element size and volume filling. Considering the force constant C as a lower bound of the inter element interaction, the main remaining uncertainty results from that on the density. It is expected to be accurate within a factor of two at high values of porosity $(1 - \emptyset)$ leading to a total uncertainty for the strength in the same order. These errors are the ones inherent in the formalism of Sec. 3.3. Further variations in strength may result from bigger variations in velocity, which we will address in the next section.

p_i	p_i^{ref}	$w_i = \left\lvert \frac{p_i}{\sigma} \cdot \frac{\Delta\sigma}{\Delta p_i} \right\rvert$
$Force\ constant\ C$ $[N/m]$	$2.6 * 10^{-2}$	1.0
$d_{c_1}[\mu m]$	10	0.025
$d_{c_2}[\mu m]$	40	0.64
c	2.39	0.23
b	0.43	0.84

Table 2: Error weighting factors w_i for a +- 1% variation of parameters p_i around a reference state p_i^{ref} (σ_{ref} = 776 Pa).

3.5 Example dust particles

In this section, we apply the various strength estimations to some example particles of Sec. 2. From their area and height we estimate an equivalent spherical diameter d_{eq} of the incoming dust agglomerates and then apply the above formalism.

Table 3 shows the resulting strength estimates from our three approaches: fragment sizes, σ_{fs} and energy density arguments, where $\sigma_{ed}^{(1)}$ is calculated for a mean impact velocity of 3.5 m/s while $\sigma_{ed}^{(2)}$ is evaluated assuming a size dependent velocity. As CF Pecine is a particle which is not fragmenting, we can only give a lower limit on strength based on the energy density arguments. 2D0 Stefanie and 2CF Pertti are examples for dust which breaks up into few pieces (diameter size range 15 to 40 μm) and 2CF Nilda is an example for complete fragmentation (diameter size range 10 to 30 μm). 2CF Lambert is big but does not fragment and again only a lower bound can be given for the strength.

In our whole data reduction we have assumed that dust particles within the size range observable by COSISCOPE (from a few 10 μm to a few 100 μm) arrive with a common velocity. This is likely if all particles up to a few 100 μm in size are lifted together from the comet's surface and break up to smaller sizes afterwards. Indeed, there is no strong evidence from GIADA for a size dependence on the velocity. However, if the differentiation already occurs during the liftoff-process then there may be a bigger spread in velocity. Theoretical models assume $v \propto d_{eq}^{-0.5}$ (Agarwal et al., 2007). In order to show the direction and the possible magnitude of the effect on strength Table 3 additionally contains energy density values for the variable velocity case $\sigma_{ed}^{(2)}$ where it is assumed that both approaches coincide at the largest observed dust particle (Nilda). It shows that for the case of simple breakup (Stefanie and Pertti) the spread of our strength estimate becomes bigger since the upper limit increases. For not-fragmenting small dust (Pecine) the lower bound for strength rises by a factor of 5, whereas for larger not-fragmenting dust (example Lambert) it roughly stays within a factor of two. High strength for small dust in the few 10 μm size range would also explain why the agglomerate "elements" survive the impacts observed up to now.

Breakup type	Example	d $[\mu m]$	h $[\mu m]$	d_{eq} $[\mu m]$	d_{c_1} $[\mu m]$	d_{c_2} $[\mu m]$	$\emptyset$	ρ $[\frac{kg}{m^3}]$	$\sigma_{ed}^{(1)}$ $[Pa]$	$\sigma_{ed}^{(2)}$ $[Pa]$	σ_{fs} $[Pa]$
No breakup	1CF Pecine	45	50	53	-	-	-	270	>1650	> 7800	-
Simple breakup	2D0 Stefanie	100	40	85	15	40	0.61	225	<1378	< 4050	>1175
Simple breakup	2CF Pertti	135	50	110	20	35	0.57	200	<1240	< 2790	>1020
Catastrophic breakup	2CF Nilda	410	120	250	10	30	0.37	147	<900	< 900	>850
No breakup, large particle	2CF Lambert	110	116	130	-	-	-	190	>1160	> 2235	-

Table 3: Strength values for some of the dust particles of Sec. 2 as derived from considerations of energy density ("ed") and fragment spectrum ("fs"). ($d = \sqrt{\frac{4}{\pi} \cdot a}$, a= area in image plane), h: height, derived from shadow; $d_{eq} =$ equivalent sphere diameter : $(\frac{3}{2} \cdot d^2 \cdot h \cdot \varepsilon)^{1/3}$, ε is a form factor of the dust. It is 1 for squared forms, 1/2 for roof shapes and 1/3 for pyramid shapes. In the above examples ε = 1 for all cases except Nilda, ε = 1/2 .

d_{c_1}, d_{c_2} : lower and upper fragment diameters; $\emptyset$: volume filling factor. ρ: incoming dust agglomerate mean density; $\sigma_{ed}^{(1)}$: strength estimate from energy density assuming a mean impact velocity of 3.5 m/s; $\sigma_{ed}^{(2)}$: strength estimate from energy density for size dependent velocity; σ_{fs} : strength estimate from analysis of fragment spectrum.

4. Discussion and summary

A first analysis of the fragmentation behavior has been performed for dust particles collected by the COSIMA instrument onboard ROSETTA for the dust collection time period Aug. 2014 to Feb. 2015, when Comet Churyumov-Gerasimenko was still on its way inbound to the Sun. Their sizes span a wide range: between some 10µm and about 400 µm. Many of them broke up upon impact, thus revealing details about their interior. We were able to derive quantitative bounds for the mechanical strength of dust particles in the near coma of a comet, for which no previous data existed.

The general trend is that the larger dust particles fragmented whereas most of the smaller ones remained undamaged. The resolution of the images down to a precision of about 10 µm enabled insights on the morphology of the undamaged dust as well as of fragmenting dust through its characteristic fragment pattern. Interestingly, the fragmented and many of the undamaged dust particles form a cluster-like aggregate resembling a bunch of grapes. The size of these sub-units has been found to be in the order of a few tens of microns and we have denoted them by "elements". The most important finding is that these cluster

“elements” distinguished in the un-fragmented dust particles are essentially within the same size range as the individual fragments dispersed after disruption of the fragmenting dust particles. This observation led us to the supposition that these elements are pre-existing and pre formed in the parent dust and simply were torn apart during the deceleration. Surely, they have their own internal substructure composed of smaller sub-micron sized granules of mixed composition.

Among the overwhelming wealth of collected samples there are few cases of larger dust particles (> 100 µm) that do not feature any damage and present only little substructure on the level of the visual resolution. As we lack information about the velocity correlated with a certain individual mass or size of the COSIMA incoming dust particles during the collecting period, we can only postulate that they might either belong to the lower part of the velocity population, having as references the speed values measured by GIADA (Rotundi et al., 2015, Della Corte et al. 2015), or possess higher density and higher strength. In a parallel paper of Langevin et al. (2015) it is shown that in several cases big impact events possibly correspond to much bigger dust particles fragmenting prior to the arrival at the gold black collecting substrate, e.g. at the walls of the entry funnel of the instrument (Kissel et al., 2009). The largest dust particles (>100 µm) generally show disruption upon collision, which implies that these particles have a lower density, a higher porosity and a weaker mechanical strength compared to smaller particles. This conclusion is in agreement with laboratory measurements of dust aggregates and with the theoretical models that predict a reduction on the value of tensile strength and the velocity threshold for disruption with increasing the aggregate’s size (Weidling et al. 2011, Meru et al 2013, Skorov et al. 2012).

For the quantitative data reduction we used very simple phenomenological concepts, which represent more of a dimensional analysis rather than being an explicit theory. The reason for this choice being the complete lack of material data as well as uncertainties in the chemical nature of the smallest building blocks at nanometer scales. Also our aim was to stay as close as possible at the data observed with a minimum of further theoretical modeling. Nevertheless we were able to estimate an order of magnitude for the mechanical strength. It was found to be in the order of 1000 Pa (for the example of a particle with $\approx$100 μm radius) with an accuracy of about a factor of two, mainly resulting from uncertainties in the estimate of the dust’s density. For fragmenting dust, energy density arguments gave an upper bound for the mechanical strength whereas the analysis of the fragment size spectrum assuming van der Waals interaction led to a lower bound. For undamaged dust particles, only a lower bound could be asserted. This lower bound can rise considerably when taking into account a possible size dependence of the velocity (Agarwal et al., 2007). Each of the three approaches, energy density, forces and van der Waals modeling has its own uncertainties and assumptions. However, all three together form a set of arguments that show a high degree of internal consistency.

The values derived here are for agglomerates of sizes up to a few 100 micrometers hitting our collection targets at low velocity. However, the inner strength of their “elements” might be much higher than the values derived here for larger agglomerates, maybe due to sticking enhancement by refractory organic material (Kudo 2002). Some substructures of IDP’s are of this size and organic glue has been found at nanometer scales (Flynn 2013, Matrajt et al., 2012). As we have previously referred (Langevin et al., 2015), many of the particles observed by COSIMA are dark, although they appear bright before the gold black’s background. The reason might be an abundance of organics. Our observation of the relative stability of fragment sizes of some tens of micrometers gives a strong argument in this direction.

Most of the dust particles collected by COSIMA are thought to have lost their volatiles, i.e. they are skeletons consisting of the remaining mineral and refractory organic components. In the presence of frozen volatiles strength values may be roughly one order of magnitude higher (Blum et al. 2014, Gundlach et al.2014, Aumatell and Wurm 2013).

For dust sizes much larger than a few 100 μm, the physics of interaction may change, being not any more described by van der Waals adhesion forces uniquely (Lee et al., 1995). For the largest objects, the comets as a whole, there exist “fragmentation experiments” conducted by nature itself as has been observed during the disruption of Shoemaker-Levy 9 by its Jupiter passage in 1992. Differential gravitational forces per surface cross sectional area have been deduced as being in the order of 10 Pa (Scotti and Melosh, 1993). Housen and Holsapple (1990) have undertaken an effort to connect data between those enormously different scale lengths by establishing a general scaling law for strength by dimensional analysis. Their basic finding is that breakup not only depends on the energy density transmitted to the objects, but also on the size of the object and the strain rate applied, which is in line with our above argument that strength has to be defined with respect to a certain fragmentation process. For strength dominated objects (sizes less than a few km) they derive an approximate scaling law for the radius dependence: $\sigma \sim r^{-\propto}$ where $0.24 < \propto < 0.5$ (Benz and Asphaug, 1999). When taking our value of 10^3 Pa (and after correction for the presence of volatiles 10^4 Pa) at 100 μm size and the Shoemaker-Levy value of 10 Pa at km size $\sigma \approx 200 \cdot r^{-0.43}$ Pa follows (for r in meters). This compares with our $r^{-0.4}$ size dependence of energy densities within our small observational window of sizes.

The present observations point to weak mechanical strength as a possible general feature of cometary matter. This is fully consistent with the very low strength (10 to 40 Pa) observed by OSIRIS at much larger scales (several 10 m through the break-up of overhangs, Groussin et al., 2015). These weak strengths at scales from a few 10 μm to several meters support the view that cometary material has undergone very little processing since accretion, with the possible exception of a higher strength sun-exposed crust. The size dependence of its material properties may not follow a continuous sequence from nanometer to bigger sizes, based on material properties on the nanometer scale alone. There might be even discontinuities at some size boundaries, when the physics of binding changes its nature. The present data indicate that the size range of a few tens of micrometers represents such a boundary.

Acknowledgments:

COSIMA was built by a consortium led by the Max-Planck-Institut für Extraterrestrische Physik, Garching, Germany in collaboration with Laboratoire de Physique et Chimie de l'Environnement et de l'Espace, Orléans, France, Institut d'Astrophysique Spatiale, CNRS/Université Paris Sud, Orsay, France, Finnish Meteorological Institute, Helsinki, Finland, Universität Wuppertal, Wuppertal, Germany, von Hoerner und Sulger GmbH, Schwetzingen, Germany, Universität der Bundeswehr, Neubiberg, Germany, Institut für Physik, Forschungszentrum Seibersdorf, Seibersdorf, Austria, Institut für Weltraumforschung, Österreichische Akademie der Wissenschaften, Graz, Austria and is lead by the Max-Planck-Institut für Sonnensystemforschung, Göttingen, Germany. The support of the national funding agencies of Germany (DLR, grant 50 QP 1302), France (CNES), Austria, Finland and the ESA Technical Directorate is gratefully acknowledged. One of the co-authors is supported by the Italian Space Agency within the ASI-INAF agreements I/032/05/0 and I/024/12/0. We thank the Rosetta Science Ground Segment at ESAC, the Rosetta Mission Operations Centre at ESOC and the Rosetta Project at ESTEC for their outstanding work enabling the science return of the Rosetta Mission.

References:

Agarwal J., Mueller M., Gruen E., 2007. Dust Environment Modelling of Comet 67P/Churyumov-Gerasimenko. Space Sci Rev 128, 79–131.

Aumatell G., Wurm G., 2014. Ice aggregate contacts at the nm-scale. Mon. Not. R. Astronom Soc. 437 (1): 690-702. Doi: 10.1093/mnras/stt1921.

Bentley M. S., Torkar K., Romstedt J., 2014. The structure of cometary dust – first results from the MIDAS Atomic Force Microscope onboard ROSETTA. AGU Fall Meeting San Francisco, paper P32B-03.

Benz W. and Asphaug E., 1999. Catastrophic Disruptions Revisited. ICARUS, vol. 142, no. 1, 5–20.

Blum J. and Wurm G., 2008. The Growth Mechanisms of Macroscopic Bodies in Protoplanetary Disks. Annu. Rev. Astro. Astrophys., vol. 46, no. 1, pp. 21–56.

Blum J., Gundlach B., Mühle S., Trigo-Rodriguez J.M., 2014. Comets formed in solar-nebula instabilities! – An experimental and modeling attempt to relate the activity of comets to their formation process. Icarus 235, 156–169.

Blum J. and Schräpler R., 2004. Structure and Mechanical Properties of High-Porosity Macroscopic Agglomerates Formed by Random Ballistic Deposition,
Phys. Rev. Letters, 93, 11.

Bower A.F., 2010. Applied Mechanics of Solids, C&C Press, Taylor and Francis.

Bradley J.P. 2013. How and where did GEMS form? Geochimica et Cosmochimica Acta 107, 336–340.

Brownlee D., 1985. Cosmic dust – Collection and research. Annu. Rev. Earth Planet. Sci., 13, 147-173.

Brownlee D., 2014. The Stardust Mission: Analyzing Samples from the Edge of the Solar System. Annu. Rev. Earth Planet. Sci. 42:179-205.

Ceplecha Z. and McCrosky R.E., 1976. Fireball end heights - A diagnostic for the structure of meteoric material. J. Geophys. Res. 81, 6257–6275.

Clark B. C., Green S.F., Economou T.E., Sandford S.A., Zolensky M.E., McBride N., Brownlee D., 2004. Release and fragmentation of aggregates to produce heterogeneous, lumpy coma streams. J. Geophys. Res. 109, E12S03, doi:10.1029/2004JE002319.

Della Corte V., Rotundi A. Fulle M., Gruen E., Weissman P., Sordini R., Ferrari M., Ivanovski S., Lucarelli F., Accolla M., Zakharov V., Mazzotta Epifani E., Lopez-Moreno J.J., Rodriguez J., Colangeli L., Palumbo P., Bussoletti E., Crifo J.F., Esposito F., Green S.F., Lamy P.L., McDonnell J.A.M., Mennella V., Molina A., Morales R., Moreno F., Ortiz J.L., Palomba E., Perrin J.M., Rietmeijer F.J.M., Rodrigo R., Zarnecki J.C., Cosi M., Giovane F., Gustafson B., Herranz M.L., Jeronim J.. Leese M.R., Lopez-Jimenez A.C., Altobelli N., 2015. GIADA: shining a light on the monitoring of the comet dust production from the nucleus of 67P/Churyumov Gerasimenko. Astronomy & Astrophysics manuscript no. aa26208-15 c ESO 2015 August 19, 2015.

Duprat J., Engrand C., Maurette M., Kurat G., Gounelle M., Hammer C., 2007. Micrometeorites from Central Antarctic snow: The CONCORDIA collection. Advances in Space Research 39, 605–611.

Engrand C., Benzerara K., Leroux H., Duprat J., Dartois E., Bardin N., Delauche L., 2015. Carbonaceous phases and mineralogy of Ultracarbonaceous Antarctic Micrometeorites identified by C- and N-XANES/STXM and TEM, 46 Lunar and Planetary Science Conference, Paper No. 1902.

Flynn G.J., Wirick S., 2, Keller L.P., 2013. Organic grain coatings in primitive interplanetary dust particles: Implications for grain sticking in the Solar Nebula. Earth Planets Space, 65, 1159–1166.

Fulle M., Della Corte V., Rotundi A., Weissman, P., Juhasz, A., Szego, K., Sordini, R., Ferrari M., Ivanovski S., Lucarelli F., Accolla M., Merouane S., Zakharov V., Mazzotta Epifani E., Lopez-Moreno J.J., Rodriguez J., Colangeli L., Palumbo P., Gr¨un E., Hilchenbach M., Bussoletti E., Esposito F., Green S. F., Lamy P. L., McDonnell J. A. M., Mennella V., Molina A., Morales R., Moreno F., Ortiz J. L., Palomba E., Rodrigo R., Zarnecki, J. C., Cosi J. M., Leese M. R., Lopez-Jimenez A. C., Altobelli N., 2015. Density and Charge of Pristine Fluffy Particles from Comet 67P/Churyumov–Gerasimenko. Astrophysical Journal Letters, 802(1): L12 (5pp).

Greenberg, J. M. and Hage J. I., 1990. From interstellar dust to comets - a unification of observational constraints. *Ap. J.* 361, 260–274.

Greenberg J. M., Li A., 1999. Morphological Structure and Chemical Composition of Cometary Nuclei and Dust. Space Science Reviews 90: 149–161.

Groussin O., Jorda L., Auger A-T. et al., 2015. Gravitational slopes, geomorphology and material strengths of the nucleus of comet 67P/Churyumov-Gerasimenko from OSIRIS observations. http://dx.doi.org/10.1051/0004-6361/201526379

Güttler C., Krause R., Geretshauser R., Speith R., Blum J., 2009. The Physics of Protoplanetesimal Dust Agglomerates. IV. Toward a Dynamical Model, The Astrophysical Journal 701,130–141. doi:10.1088/0004-637X/701/1/130

Gundlach B. and Blum J., 2014. The stickiness of micrometer sized water-ice particles, The Astrophysical Journal 798, 1. http://dx.doi.org/10.1088/0004-37X/798/1/34.

Hilchenbach M., et al., 2015. Comet 67P/Churyumov-Gerasimenko - Close-Up on Dust Particle Fragments. To be submitted to ApJL

Hornung K., Kissel J., Fischer H., Mellado E.M., Kulikov O., Hilchenbach M., Krüger H., Engrand C., Langevin Y., Rossi M., Krueger F.R., 2014. Collecting cometary dust particles on metal blacks with the COSIMA instrument onboard ROSETTA. Planetary and Space Science 103, 309–317.

Hornung K. and Kissel J., 1994. On shock wave ionization of dust particles, Astron. Astrophys. 291,324-336.

Housen K.R. and Holsapple K.A., 1990. On the fragmentation of asteroids and planetary satellites, ICARUS 84, 226–253.

Israelachvili J.N., 2011.Intermolecular and Surface Forces, Academic Press, 3rd. Edition.

Kirchner H., Michot G., Schweizer J., 2002. Fracture toughness of snow in shear and tension, Scripta Materialia, 46, 6, 425–429.

Kissel J., Glasmachers A., Grün E., Henkel H., Höfer H., Haerendel G., v.Hoerner H., Hornung K., Jessberger E.K., Krueger F.R., Möhlmann D., Greenberg J.M., Langevin Y., Silen J., Brownlee D., Clark B.C., Hanner M.S., Hoerz F., Sandford S., Sekanina Z., Tsou P., Utterback N.G., Zolensky M.E., Heiss C., 2003. Cometary and Interstellar Dust Analyzer for comet Wild 2. Journal of Geophysical Research 108, E10, 8114.

Kissel, J., COSIMA Team, 2009. COSIMA: High resolution time-of-flight secondary ion mass spectrometer for the analysis of cometary dust particles onboard ROSETTA. In:Schulz R.,Alexander C.,Boenhardt H.,Glassmeier K.H.(Eds.), ESA's Mission to the Origin of the Solar System. Springer,NewYork, 201–242.

Kudo T., Kouchi A., Arakawa M., Nakano H., 2002. The role of sticky interstellar organic material in the formation of asteroids. Meteoritics & Planetary Science 37,1975-1983.

Langevin Y., Hilchenbach M., Ligier N., Merouane S., Hornung K., Engrand C., Schulz R., Kissel J., Ryno J. and the COSIMA team, 2015. Typology of dust particles collected by the COSIMA mass spectrometer in the inner coma of 67P/Churyumov Gerasimenko. Submitted to Icarus Aug. 2015.

Lee L.H., 1995. Adhesion and cohesion mechanics of lunar dust on the moon's surface. J. of Adhesion Science and Technology 9, 8, 1103-1124.

Maas D., Krueger F.R., Kissel J., 1990. Mass and Density of Silicate- and CHON-Type Dust Particles Released by Comet P/Halley. Asteroids, Comets, Meteors III, Proceedings of a meeting (AMC 89) held at the Astronomical Observatoy of the Uppsala University, Ed. C.I. Lagerquist, H. Rickman B.A: Lindblad, p. 389 ff.

Matrajt G., Messenger S., Brownlee D., Joswiak, D., 2012. Diverse forms of primordial organic matter identified in interplanetary dust particles. Meteoritics & Planetary Science 47, 4, 525–549. doi: 10.1111/j.1945-5100.2011.01310.x

Meru F., Geretshauser R.J., Schaefer Ch., Speith R., Kley W., 2013.
Growth and fragmentation of centimetre-sized dust aggregates: the dependence on aggregate size and porosity. Mon. Not. R. Astronom. Soc. 435, p.2371.

Riedler W. et al., 2007. MIDAS The Micro-Imaging Dust Analysis System for the Rosetta Mission. Space Sci. Rev. 128, 869-904.

Rotundi A. et al., 2015. Dust measurements in the coma of comet 67P/Churyumov-Gerasimanko inbound to the Sun. Science 347, Issue 6220, aaa3905.

Schulz R., Hilchenbach M., Langevin Y., Kissel J., Silen J., Briois Ch., Engrand C., Hornung K., Baklouti D., Bardyn A., Cottin H., Fischer H., Fray N., Godard M., Lehto H., Le Roy L., Merouane S., Orthous-Daunay F.-R., Paquette J., Rynö J., Siljeström S., Stenzel O., Thirkell L., Varmuza K., Zaprudin B., 2015. Comet 67P/Churyumov-Gerasimenko sheds dust coat accumulated over the past four years. Nature 518, 216-218. doi:10.1038/nature14159.

Skorov Yu. and Blum J., 2012, Dust release and tensile strength of the non-volatile layer of cometary nuclei. Icarus 221,(1),1–11.

Scotti J.V., Melosh H.J., 1993. Estimate of the size of comet Shoemaker-Levy 9 from a tidal breakup model. Nature 365, 6,733–735.

Thomson R.M., 1973. The fracture crack as an imperfection in a nearly perfect solid, Annual Review of Materials Science, 3, 31-51.

Weidling, R., Güttler, C., Blum, J., 2012. Free Collisions in a Microgravity Many-Particle Experiment. I. Dust Aggregate Sticking at Low Velocities. Icarus, 218, 688-700.

Highlights

- We collected dust in the near coma of Comet 67P/Churyumov-Gerasimenko.
- Dust particles > 100 micrometers fragment upon impact on our collection plates at velocities of a few m/s.
- The dust consists of smaller elements (few tens of micrometers) that remain intact during impact.
- An order of magnitude for strength is derived (e.g. 1000 Pa for 100 micrometer sized fragmenting dust).
- The mechanical properties of cometary matter change with size, possibly in a non-continuous way, due to changing binding mechanisms.

Graphical abstract: